

RESEARCH ARTICLE

Retinoic acid regulates size, pattern and alignment of tissues at the head-trunk transition

Keun Lee* and Isaac Skromne[†]**ABSTRACT**

At the head-trunk transition, hindbrain and spinal cord alignment to occipital and vertebral bones is crucial for coherent neural and skeletal system organization. Changes in neural or mesodermal tissue configuration arising from defects in the specification, patterning or relative axial placement of territories can severely compromise their integration and function. Here, we show that coordination of neural and mesodermal tissue at the zebrafish head-trunk transition crucially depends on two novel activities of the signaling factor retinoic acid (RA): one specifying the size and the other specifying the axial position relative to mesodermal structures of the hindbrain territory. These activities are each independent but coordinated with the well-established function of RA in hindbrain patterning. Using neural and mesodermal landmarks we demonstrate that the functions of RA in aligning neural and mesodermal tissues temporally precede the specification of hindbrain and spinal cord territories and the activation of *hox* transcription. Using cell transplantation assays we show that RA activity in the neuroepithelium regulates hindbrain patterning directly and territory size specification indirectly. This indirect function is partially dependent on Wnts but independent of FGFs. Importantly, RA specifies and patterns the hindbrain territory by antagonizing the activity of the spinal cord specification gene *cdx4*; loss of *Cdx4* rescues the defects associated with the loss of RA, including the reduction in hindbrain size and the loss of posterior rhombomeres. We propose that at the head-trunk transition, RA coordinates specification, patterning and alignment of neural and mesodermal tissues that are essential for the organization and function of the neural and skeletal systems.

KEY WORDS: Retinoic acid, *cdx*, Hindbrain, Spinal cord, Patterning, Head-trunk transition, Craniovertebral junction, Zebrafish

INTRODUCTION

The coherent organization of the neural and skeletal systems requires that the respective neuroectodermal and mesodermal precursor tissues align accurately along the vertebrate rostrocaudal axis. Changes in the axial position of precursor tissues can result in structural malformations and compromised function. Alignment is particularly crucial at the head-trunk transition, where the basal opening of the occipital bone, the foramen magnum, must align with the caudal hindbrain to allow the nerve cord safe passage into the vertebral canal. Both misalignments and structural abnormalities have long been known to result in severe neurological syndromes (List, 1941; Marin-Padilla, 1991). Although significant progress has

been made in understanding neural and mesodermal regionalization (reviewed by Stern et al., 2006), the mechanisms specifying the relative position of neural and mesodermal tissues within the vertebrate rostrocaudal axis remain unknown. Here, we set out to study the earliest processes involved in neural and skeletal system integration by investigating the signaling events that specify the rostrocaudal position and relative alignment of hindbrain/spinal cord (HB/SC) territories to the somitic precursors of the head and trunk bones and muscles.

Specification events that regionally restrict the identity of neural progenitor cells to a hindbrain or spinal cord fate would necessarily specify the rostrocaudal position of the HB/SC transition. The hindbrain and spinal cord are specified from a common progenitor tissue, the caudal neural plate (Schoenwolf, 1992; Muhr et al., 1997, 1999; Brown and Storey, 2000), through the binary activity of *Cdx* transcription factors (Skromne et al., 2007). Transcription of *cdx* genes in the caudal neural plate is initially broad, but is quickly turned off rostrally to allow hindbrain segmentation and patterning, while it is maintained in the ‘on’ state caudally to specify spinal cord (Skromne et al., 2007; Sturgeon et al., 2011). These events take place from mid-gastrulation to early segmentation (Muhr et al., 1997, 1999; Woo and Fraser, 1998; Nordström et al., 2006; Skromne et al., 2007; Sturgeon et al., 2011) and are crucial for proper cell fate allocation. In mouse and zebrafish, changes in the expression domain of *cdx* changes the size of the hindbrain and spinal cord territories in a reciprocal manner; a rostral expansion of *cdx* transcriptional domain reduces the hindbrain and expands the spinal cord, whereas a caudal reduction in *cdx* transcriptional domain expands the hindbrain and reduces the spinal cord (Charite et al., 1998; Shimizu et al., 2006; Skromne et al., 2007; van Rooijen et al., 2012). Thus, in order to understand the processes that establish the position of the HB/SC transition, it is important to understand the mechanisms of *cdx* regulation.

Regulation of *cdx* genes is complex, with several signaling factors influencing transcription. All three members of the *cdx* family of transcription factors, *cdx1*, *cdx2* and *cdx4*, are transcribed in the caudal region of embryos (Frumkin et al., 1991; Gamer and Wright, 1993; Meyer and Gruss, 1993; Beck et al., 1995; Skromne et al., 2007). This restricted caudal expression is controlled by the activity of the signaling factors FGF, Wnt and retinoic acid (RA) (reviewed by Lohnes, 2003; Deschamps and van Nes, 2005). Whereas the regulatory function of these signals on *cdx* transcription has been extensively studied in the context of mesoderm anterior-posterior patterning (reviewed by Deschamps and van Nes, 2005), the regulation of *cdx* in nervous system regionalization has not been characterized.

RA is a suitable candidate to regulate both *cdx* expression in neural tissue and the axial placement of the HB/SC transition relative to the paraxial mesoderm. In all species examined, RA is synthesized at the right place and time, the paraxial mesoderm adjacent to the HB/SC transition (Niederreither et al., 1997;

Department of Biology, University of Miami, Coral Gables, FL 33146, USA.

*Present address: University of Miami Miller School of Medicine, 1301 Memorial Drive, Coral Gables, FL 33146, USA.

[†]Author for correspondence (iskromne@bio.miami.edu)

Swindell et al., 1999; Begemann et al., 2001; Grandel et al., 2002), during the hindbrain and spinal cord specification period (Woo and Fraser, 1998; Muhr et al., 1999). Importantly, RA can induce caudal neural plate explants fated to become posterior spinal cord to change their *hox* expression profile to that of more anterior regions (Nordström et al., 2006). Whereas changes in spinal cord gene expression from posterior to anterior could be attributed to the well-known function of RA in *hox* patterning gene regulation (Sockanathan and Jessell, 1998; Liu et al., 2001; reviewed by Glover et al., 2006; Rhinn and Dolle, 2012), patterning processes alone cannot explain the transformation of spinal cord to hindbrain identities. Instead, the transformation suggests that, in addition to its patterning functions, RA is also involved in hindbrain and spinal cord specification.

In this study we demonstrate a novel role for RA in specifying the axial position and alignment of the HB/SC transition relative to mesodermal tissues in zebrafish. These activities depend on Cdx4 and can be distinguished from RA patterning functions temporally and mechanistically. Temporally, timed inhibition of RA activity demonstrates that RA aligns the neural and mesodermal tissue early during gastrulation, before the specification of hindbrain and spinal cord territories, and the expression of *hox* patterning genes. Mechanistically, cell transplantation approaches show that RA induces posterior patterning genes in the hindbrain directly, but functions in regulating *cdx4* spatial expression domain indirectly. The indirect regulation of *cdx4* through RA is FGF-independent, but requires Wnt activity. Together, these findings identify RA as a key component in the signaling network regulating the specification, alignment and patterning of hindbrain, spinal cord and mesodermal tissues that are essential for the functional organization of nervous and skeletal systems at the head-trunk transition.

RESULTS

RA regulates hindbrain size specification and neural-to-mesodermal alignment at the head-trunk transition

To investigate the processes aligning neural to mesodermal tissues at the head-trunk transition, we analyzed the axial position of hindbrain, spinal cord and mesodermal landmarks in zebrafish embryos lacking RA. RA is a suitable candidate to mediate tissue alignment, as changes in RA levels cause hindbrain defects and spinal cord mis-patterning (Begemann et al., 2001; Grandel et al., 2002; Emoto et al., 2005). In considering landmarks for analysis, we focused on two commonly used markers to analyze changes in hindbrain specification (Begemann et al., 2001; Grandel et al., 2002; Emoto et al., 2005; Maves and Kimmel, 2005): the rostral border of rhombomere 3 (r2/r3), as identified by expression of *krx20* (Oxtoby and Jowett, 1993), and the somites identified by expression of *myoD* (Weinberg et al., 1996). With these landmarks we compared the location of the HB/SC transition, identified by the expression of the spinal cord marker *cdx4* (Skromne et al., 2007). In wild-type embryos, *cdx4* expression domain during early segmentation stages extends caudally from the somite 2/3 border (s2/s3) (Fig. 1A), which in zebrafish corresponds to occipital to vertebral somite transition (Morin-Kensicki et al., 2002). By contrast, embryos exposed at the onset of gastrulation to the RA-synthesis inhibitor DEAB, referred to hereafter as RA-deficient embryos, had both spinal cord and somites shifted rostrally closer to the r2/r3 boundary (Fig. 1B). Importantly, however, the spinal cord shifted rostrally to a greater extent than the paraxial mesoderm (Fig. 1B). This spinal cord expansion was accompanied by an equivalent hindbrain reduction, determined by the relative position of the most posterior rhombomere in these embryos, r4, to the r2/r3

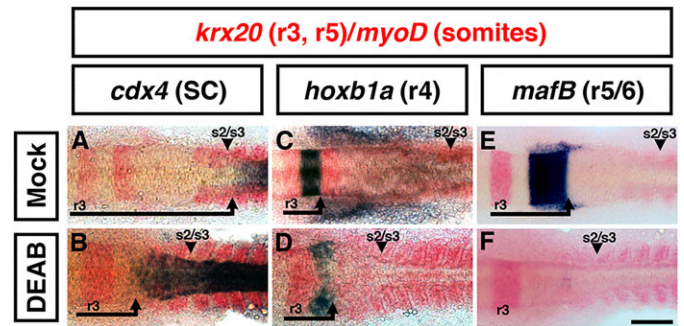


Fig. 1. RA regulates the axial position of the HB/SC transition. (A,B) RA inhibition shifts *cdx4* expression domain (purple) rostrally relative to r2/r3 (*krx20*, r3/r5 red) and somites (*myoD*, red). (C,D) RA inhibition expands the expression of the r4 marker *hoxb1a* caudally. (E,F) RA inhibition eliminates the expression of the r5/r6 marker *mafB*. Embryos at 12-somite stage are shown dorsal view, anterior to the left. Arrows, distance from r2/r3 border to relevant marker; arrowheads, somites 2/3 border. Scale bar: 50 μ m.

landmark (Fig. 1C–F). Thus, in addition to its role in rhombomere specification (Begemann et al., 2001; Grandel et al., 2002; Linville et al., 2004; Emoto et al., 2005), RA is also involved in hindbrain size specification, and in the accurate alignment of the HB/SC transition to the craniovertebral junction.

Rostrocaudal specification of hindbrain/spinal cord transition and its alignment to the craniovertebral junction are temporally distinct processes

To begin understanding the relationship between the positioning and alignment functions of RA, we asked whether these two processes require RA at the same critical period. Differences in critical periods would suggest that regulation of tissue position and

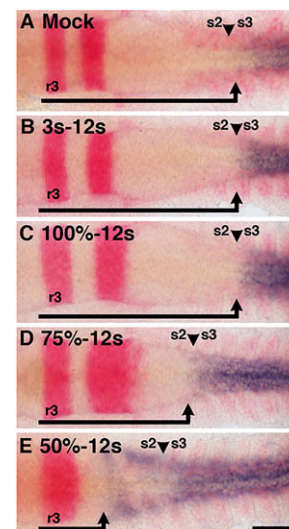


Fig. 2. Hindbrain size specification, patterning and axial alignment to mesoderm tissues are distinct temporal events. (A) Control embryos (Mock, DMSO at 50% epiboly) showing the expression of *cdx4* (purple) relative to r3 (*krx20*, red) and s2/s3 (*myoD*, red). (B,C) RA inhibition (DEAB) after gastrulation does not affect *cdx4* expression. (D) RA inhibition starting at mid-gastrulation stages (75% epiboly) shifts *cdx4* expression domain rostrally relative to r3 but not s2/s3. (E) RA inhibition starting at the onset of gastrulation (50% epiboly) shifts *cdx4* expression domain rostrally relative to r2/r3 and s2/s3. Embryos at 12-somite stage are shown dorsal view, anterior to the left. Arrows, distance from r2/r3 border to *cdx4* expression domain; arrowheads, somites 2/3 border. Scale bar: 50 μ m.

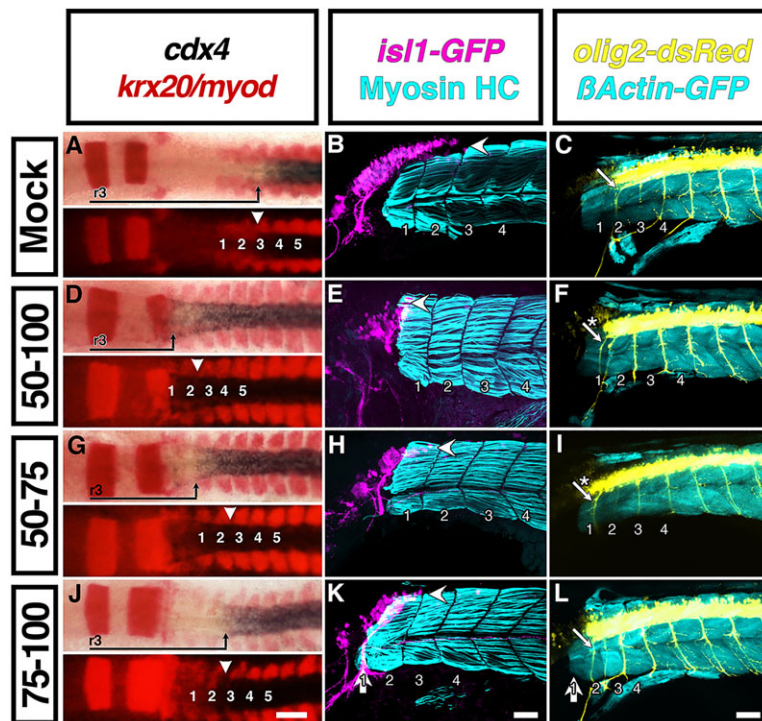


Fig. 3. RA is required early in gastrulation for neural and mesodermal tissue alignment. (A–C) Control embryos showing the expression domain of *cdx4* (purple) relative to r2/r3 boundary (*krx20*, red) and somites (*myoD*, red) early (A), and the position of branchial motor neurons (BMN, *Tg[isl1:GFP]*, magenta; B) and spinal motor neurons (SMN, *Tg[ollg2:dsRed]*, yellow; C) relative to trunk musculature (cyan) late. (D–F) RA inhibition during gastrulation (50–100% epiboly) shifts *cdx4* expression domain rostrally relative to r2/r3 and s2/s3 (D), severely reducing BMN size (E) and rostrally shifting the position of the first SMN (F). (G–I) RA inhibition during the first half of gastrulation (50–75% epiboly) shifts *cdx4* expression domain rostrally relative to r2/r3 and s2/s3 (G), severely reducing BMN size (H) and rostrally shifting the position of the first SMN (I). (J–L) RA inhibition during the second half of gastrulation (75–100% epiboly) shifts *cdx4* expression domain rostrally relative to r2/r3 while maintaining s2/s3 alignment (J), reducing BMN size (K) without affecting the first SMN position (L). Embryos in A, D, G and J are at 12-somite stage, dorsal view and anterior to the left, shown under bright-field and epifluorescent illumination to highlight somites. In these embryos, arrows indicate the distance from r2/r3 to *cdx4* expression domain, and arrowheads indicate the somites (s) 2/3 border. The remaining embryos are at 50 h post fertilization (hpf), lateral view, anterior to the left. In these embryos arrowheads indicate BMN posterior extent; small arrows, first SMN axons; asterisks, rostrally shifted SMN; large arrow, an abnormally small first somite. Numbers correspond to somites. Scale bars: 50 μ m.

alignment are separate processes. The temporal requirement of RA was analyzed by blocking RA synthesis before (50% epiboly), midway (75% epiboly) and after (100% epiboly) the gastrulation period. RA elimination after gastrulation did not change *cdx4* expression pattern (Fig. 2A–C), indicating that RA is required before segmentation for correct tissue positioning and alignment. By contrast, RA elimination at mid-gastrulation shifted both spinal cord and somites rostrally to the same extent (Fig. 2D), maintaining the alignment of tissues despite the reduction in hindbrain size. This result was different from the misalignment of neural and mesodermal tissues observed in embryos lacking RA from the beginning of gastrulation (Fig. 1B, Fig. 2E), suggesting that RA is required throughout gastrulation to specify the hindbrain territory, but only during the first half of gastrulation for correct tissue alignment. Significantly, these results show that hindbrain territory size specification and its alignment to somites are two temporally distinct and separate RA-dependent processes.

To further narrow down the temporal requirement of RA on tissue specification and alignment, we eliminated RA over short time windows. First, we confirmed that RA activity is restricted to gastrulation by exposing embryos to the inhibitor during this developmental period (50–100% epiboly), which caused phenotypic defects indistinguishable from those observed in embryos exposed to the RA inhibitor throughout development (Fig. 2E, Fig. 3D). We then blocked RA synthesis during the first (50–75% epiboly) or second (75–100% epiboly) half of gastrulation. In both conditions the size of the hindbrain was reduced, but to a lesser extent than when RA synthesis was inhibited throughout gastrulation (Fig. 3G, J). This confirmed that RA is required throughout gastrulation for hindbrain size specification. By contrast, only RA inhibition during the first half of gastrulation resulted in tissue misalignment (Fig. 3G). This is consistent with the misalignments observed in embryos exposed to the inhibitor before but not midway through gastrulation (Fig. 2D, E). Together, these results show two temporally distinct and overlapping RA activities at the HB/SC transition: RA is necessary early in gastrulation for the alignment of

neural and mesodermal tissues, and throughout gastrulation for the specification of the hindbrain territory size.

RA is required during gastrulation for the proper configuration of neural, muscular and skeletal elements at the head-trunk transition

We next investigated whether the changes in gene expression observed in RA-deficient embryos caused anatomical defects by analyzing the position of branchial and spinal motor neuron populations (BMN and SMN) relative to trunk musculature (Fig. 3) and bone structures (Fig. 4). In wild-type embryos, the last BMN population localizes as far posterior as the s2/s3 border, and the first SMN localizes at s2 (Fig. 3B, C). By contrast, loss of RA during the first half or throughout gastrulation shifts the position of both populations anteriorly by one somite (Fig. 3E, F, H, I), consistent with the rostral shifts in *cdx4* expression observed earlier in development (Fig. 3D, G). Significantly, RA inhibition late in gastrulation does not change *cdx4* expression domain or the position of motor neuron populations (Fig. 3J–L). Together, change in motor neuron position further supports the role of RA in neural and mesodermal tissue alignment.

We also analyzed the relationship between BMN and skeletal tissues by monitoring ossification events in live specimens over time, using calcein as indicator of calcium deposits (Du et al., 2001). Embryos expressing an RFP transgene in BMN (*Tg(zCREST1[isl1]:membrFP*; Mapp et al., 2010) were exposed to RA synthesis inhibitor during the first half of gastrulation, as this treatment results in neural and mesodermal tissue misalignment without causing severe hindbrain patterning defects (Fig. 3G–I). Then, from day 7 to day 14 post fertilization (dpf), we monitored changes in two bone-related parameters. First, we measured the distance along the axis from the vagal foramen in the neurocranium (identified in confocal images as the site where vagal axons cross the calcifying otic capsule; Fig. 4, white arrowheads), to the cleithrum in the pectoral girdle (Fig. 4, black arrowheads). At 10 and 12 dpf, this distance was not statistically different in wild-type ($53.83 \pm 6.28 \mu\text{m}$, $n=4$)

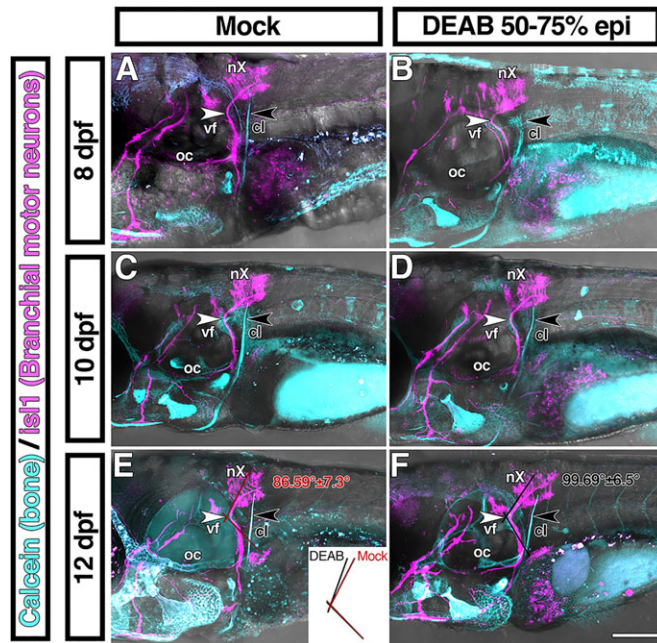


Fig. 4. RA is required for the proper configuration of neural and skeletal elements at the head-trunk transition. (A,C,E) Mock control embryos showing the position of bone structures (calcein stain, cyan) relative to branchial motor neurons (*Isl1*-RFP-positive cells, magenta) at 8 (A), 10 (C) and 12 (E) days post fertilization (dpf). (B,D,F) Stage-matched sibling embryos exposed to the RA synthesis inhibitor DEAB during the first half of gastrulation (DEAB, 50–75% epiboly). Embryos are shown lateral view, anterior to the left. White arrowhead, vagal foramen (vf); black arrowhead, cleithrum (cl); oc, otic capsule. Lines in E and F indicate the angle at which cranial nerve X (nX) axons enter and exit the vagal foramen, and are juxtaposed in panel E insert. Scale bar: 50 μ m.

and RA-deficient embryos ($53.14 \pm 6.96 \mu\text{m}$, $n=4$), suggesting preservation of the skull-to-trunk skeletal organization. We also measured the angle at which the vagal nerve enters and then exits the vagal foramen (e.g. Fig. 4E,F), as changes in this angle would suggest a shift in the position of neural populations relative to skeletal structures. At 10 and 12 dpf, this angle in wild-type embryos was $86.59^\circ \pm 7.33^\circ$, whereas in RA-deficient embryos it was $99.69^\circ \pm 6.5^\circ$ ($n=6$ per condition, t -test, $P \leq 0.0015$), suggesting a relative displacement of neural and skeletal elements. These late morphological changes are consistent with the early gene expression changes, further supporting the role of RA in head-trunk tissue alignment.

The rostrocaudal position of the hindbrain/spinal cord transition regulates rhombomere size and number

The observation that RA specifies the axial position of the HB/SC transition (Figs 2 and 3) and rhombomere identities (Begemann

et al., 2001; Grandel et al., 2002; Maves and Kimmel, 2005) over the same critical period raises the possibility that these two processes are developmentally related. There are three distinct ways in which these processes could be related. First, rhombomere specification determines the axial position of the HB/SC transition. Second, axial specification of the HB/SC transition determines the size of the hindbrain primordium and, consequently, the number and size of the rhombomeres. A final possibility is that RA regulates these processes independently but in a coordinated manner.

To test the possibility that rhombomere specification determines the axial position of the transition, we analyzed the expression domain of the spinal cord marker *cdx4* in embryos lacking *hnf1ba* (*vhnf1*, *tcf2*), a direct, early RA target gene that is essential for r5–r7/8 development (Fig. 5A–D; Sun and Hopkins, 2001; Wiellette and Sive, 2003; Hernandez et al., 2004; Pouilhe et al., 2007). If the axial position of the HB/SC transition is dependent on the formation of posterior rhombomeres, then their loss in *hnf1ba* embryos should shift the HB/SC transition rostrally. This, however, was not the case; *cdx4* was expressed in the same spatial pattern in wild-type and *hnf1ba* mutants (Fig. 5E,F). Thus, rhombomere specification does not regulate the positioning of the HB/SC transition along the embryonic axis.

We next tested the possibility that the axial position of the transition determines the size of the hindbrain primordium and, consequently, rhombomere number and size, by examining whether the loss of posterior rhombomeres in RA-deficient embryos could be rescued by caudally shifting the axial position of the HB/SC transition. To caudally shift the HB/SC transition we eliminated the activity of the spinal cord specification gene *cdx4* (Skromme et al., 2007). Because in these embryos the expression of *cdx4* cannot be used to locate the HB/SC transition, we used instead the position of the last BMN (vagus, nX) in r7/8 and the first SMN in s2. Compared with control siblings, *Cdx4*-deficient embryos had a hindbrain that appeared to be patterned normally (Fig. 6D), but which was larger in size due to a caudal expansion of r7/8 (nX; Fig. 6E,F). These embryos also had a caudally shifted spinal cord, as indicated by the localization of the first SMN to s3 (Fig. 6F). By contrast, loss of RA early in gastrulation caused an overall reduction in hindbrain size, a reduction in the size of the last BMN population and a rostral shift in the position of the first SMN to s1 (Fig. 6G–I). Remarkably, loss of *Cdx4* in an RA-deficient embryo greatly expanded the hindbrain, rescuing posterior rhombomeres and BMN (Fig. 6J,K), suggesting that posterior rhombomeres can develop in the absence of RA when the hindbrain territory is enlarged. In addition, loss of *Cdx4* in an RA-deficient embryo restored the position of the first SMN to s2, suggesting antagonistic effects of *Cdx4* and RA in SMN positioning. Together, these results show that *Cdx4* and RA regulate the axial position of the HB/SC transition, which constrains the size of the hindbrain primordium that can subsequently be specified into rhombomeres.

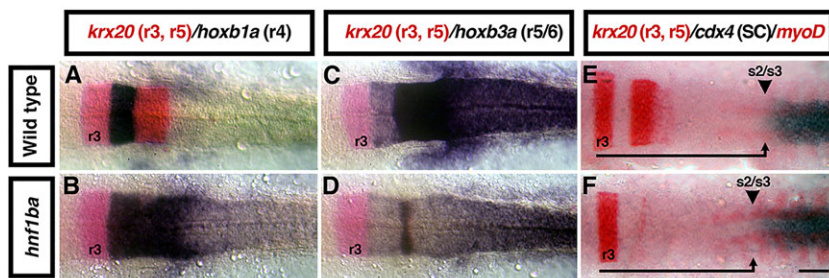


Fig. 5. Hindbrain specification and alignment are independent of hindbrain patterning. Expression analysis of hindbrain and spinal cord identity genes (purple) relative to r2/r3 (*krx20*, red) and s2/s3 (*myoD*, red) landmarks, in wild-type (A,C,E) and *hnf1ba* (B,D,F) mutant embryos. (A,B) Loss of *hnf1ba* expands the r4 marker *hoxb1a* caudally. (C,D) Loss of *hnf1ba* severely disrupts expression of the r5/r6 marker *hoxb3a*. (E,F) Loss of *hnf1ba* does not affect *cdx4* expression domain relative to r2/r3 (arrow) or s2/s3 (arrowhead). Embryos are 12-somite stage, dorsal view, anterior to the left. Scale bar: 50 μ m.

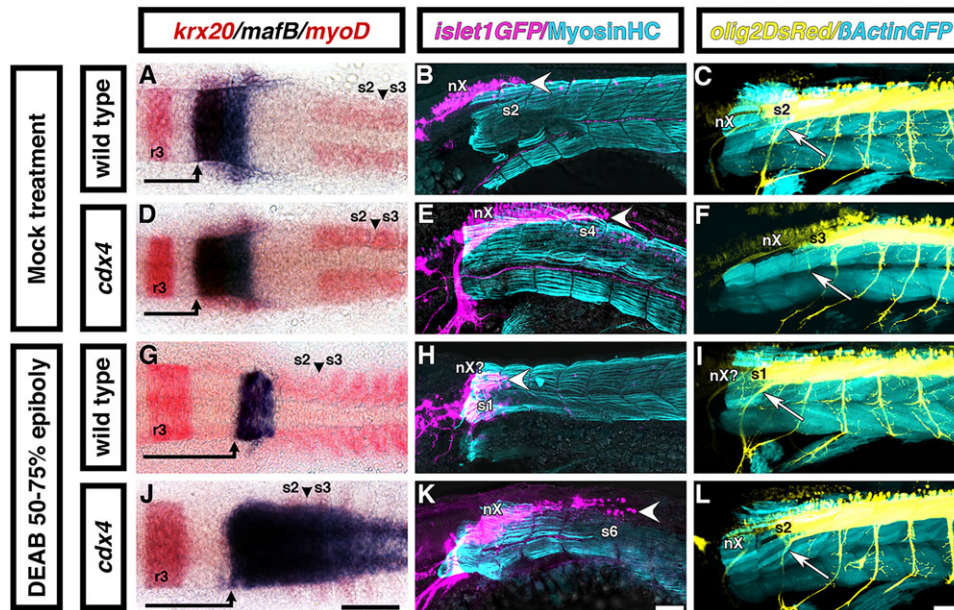


Fig. 6. Spinal cord specification constrains hindbrain territory size and rhombomere development. Analysis of r5/r6 marker *mafB* (A,D,G,J; purple), branchial (BMN; *Tg[is1:GFP]*, magenta; B,E,H,K) and spinal (SMN; *Tg[olig2:DsRed]*, yellow; C,F,I,L) motor neurons in *Cdx4*- and RA-deficient embryos. (A–C) Wild-type embryos. (D–F) *Cdx4*-deficient embryos showing wild-type *mafB* expression (C), caudally expanded nX and caudally shifted SMN (E,F). (G–I) RA loss during the first half of gastrulation (50–75% epiboly) reduces *mafB* expression domain (G) and BMN (H), and rostrally shifts the first SMN (I). (J–L) *Cdx4*/RA-double deficient embryos have a caudally expanded *mafB* expression domain (J) and BMN (K), and a normally placed first SMN (L). Embryos at 12-somite stage are shown in dorsal view, anterior to the left (A,D,G,J). Remaining embryos are 50 hpf, lateral view, anterior to the left. Black arrows, distance from s2/s3 to *cdx4* expression domain; black arrowheads, s2/s3 border; white arrowheads, posterior limit of nX; white arrows, first SMN. Scale bars: 50 μ m.

RA regulates hindbrain patterning directly and rostrocaudal position of the hindbrain/spinal cord transition indirectly

The function of RA in positioning and aligning the HB/SC transition relative to other tissues could be direct or indirect. Whereas RA is known to regulate rhombomere specification genes directly (e.g. *vhfl1*, *hox*; Serpente et al., 2005; Pouilhe et al., 2007), it can also regulate mesodermal gene expression, particularly secreted factors that can pattern the neuroectoderm, indirectly (e.g. FGF and Wnt; Muhr et al., 1997; Ensini et al., 1998; Muhr et al., 1999; Nordström et al., 2002; Nordström et al., 2006; Zhao and Duyster, 2009). To distinguish between direct and indirect functions, we combined gene overexpression and cell transplantation approaches to inactivate RA signaling exclusively in presumptive hindbrain cells while leaving RA signaling in other tissues intact. Cells from donor embryos labeled with GFP and made unresponsive to RA by overexpressing the RA-metabolizing enzyme *Cyp26c1* (supplementary material Fig. S1; Kudoh et al., 2002; Taimi et al., 2004) were transplanted into the prospective hindbrain of wild-type hosts and then analyzed for changes in gene expression. Because regulation of posterior rhombomere genes requires RA (Hernandez et al., 2004; Serpente et al., 2005; Pouilhe et al., 2007), RA-unresponsive cells should not express posterior rhombomere genes and instead express anterior rhombomere genes, similar to RA-deficient embryos (Fig. 1). Transplanted wild-type and RA-unresponsive cells populated the host neural tube to the same extent (Fig. 7D–F,K), indicating that neither transplantation nor mRNA injection procedures affected their development. However, whereas wild-type cells expressed genes appropriate to their location (Fig. 7A,D,G), RA-unresponsive cells located in posterior rhombomeres expressed genes of more anterior rhombomeres (Fig. 7C,F,I). These changes in expression were only seen in clusters of cells and not in isolated cells (95% of clones, 2% of isolated cells), presumably because only clustered cells can effectively degrade RA and prevent pathway activation. For

example, transplanted wild-type cells only expressed the r5/r6 marker *mafB* when located in r5/r6 (Fig. 7A,D,G). By contrast, transplanted RA-unresponsive cells located in r5/r6 never expressed *mafB* (Fig. 7B,E,H) and instead expressed the r4 gene *hoxb1a* (Fig. 7C,F,I), a rostral transformation similar to the ones observed in RA-deficient embryos (Fig. 1; supplementary material Fig. S1). These results show that in the posterior hindbrain, RA regulates rhombomere identity directly.

The effect of RA in regulating hindbrain and spinal cord specification was then tested by analyzing the expression of the spinal cord marker *cdx4* in RA-unresponsive cells. If RA directly regulates the axial position where the hindbrain ends and the spinal cord begins, then local RA pathway inactivation should transform the identity of neural cells in one territory to the identity of the other territory, thus altering *cdx4* expression profile. Significantly, *cdx4* expression did not change in RA-unresponsive cells irrespective of clone size or location; RA-unresponsive cells did not express *cdx4* in the hindbrain and continued to express *cdx4* in the spinal cord (100% clones in 20 embryos, Fig. 7J–L). These observations indicate that RA function in *cdx4* regulation and in hindbrain and spinal cord specification is indirect.

RA is necessary but insufficient for the alignment of the hindbrain/spinal cord transition to the mesoderm

Thus far our results suggest that RA acting indirectly is necessary for hindbrain and spinal cord specification, and presumably for their alignment to the mesoderm. To test whether RA is sufficient for neural and mesodermal alignment, we increased RA levels by exposing embryos at 50% epiboly to either a pan-inhibitor of RA degradation enzyme *Cyp26* or to RA and analyzed the expression of *krx20* in r3/r5, *hoxb4a* in r7/8 and *cdx4* in spinal cord. Consistent with previous reports, increasing RA transformed the hindbrain anterior identities to posterior fates (Fig. 8A,B; Hill et al., 1995;

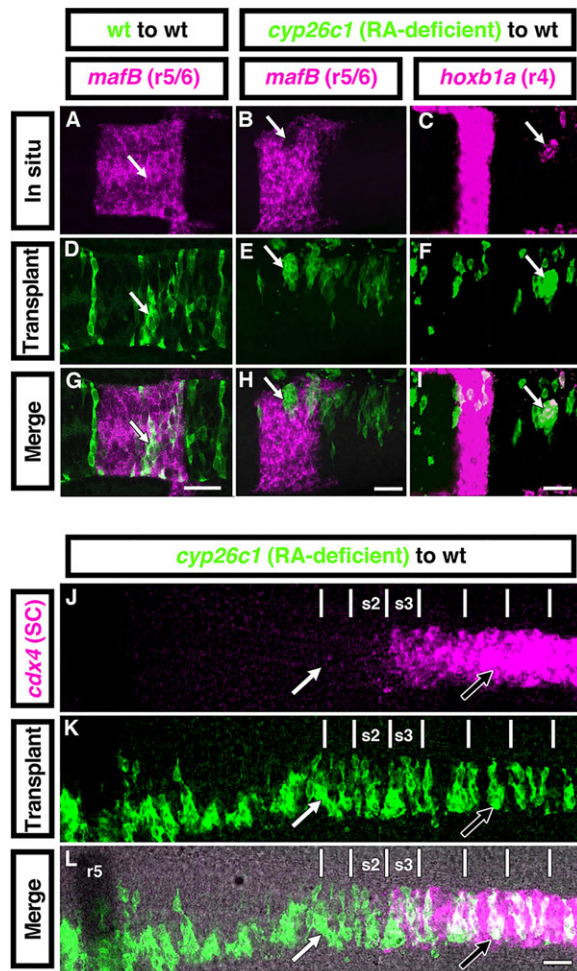


Fig. 7. Retinoic acid regulates hindbrain patterning directly and axial position indirectly. Expression analysis of hindbrain and spinal cord markers (magenta) in wild-type (A,D,G) or RA-deficient (Cyp26c1-overexpressing; B,C,E,F,H-L), GFP-positive cells transplanted into wild-type host. (A,D,G) Wild-type clones express *mafB* when located in r5/r6 (arrow, $n=5/5$ clones, $n=5$ embryos). (B,E,H) RA-deficient clones do not express *mafB* when located in r5/r6 (arrow; $n=3/3$ clones, $n=3$ embryos). (C,F,I) RA-deficient clones express the r4 marker *hoxb1a* when located in r5/r6 (arrow; $n=3/4$ clones, $n=4$ embryos). (J,K,L) RA-deficient clones express *cdx4* in the spinal cord (black arrow; $n=35/35$ clones, $n=20$ embryos) and not in the hindbrain (white arrow; $n=32/32$ clones, $n=20$ embryos). Embryos in J–L were counterstained with *kx20* (black) to visualize rhombomere 5 (r5), and with DAPI to visualize somite (s) boundaries (not shown; white lines). Embryos are 12-somite stage, dorsal side up, anterior to the left. Scale bars: 50 μm.

Begemann et al., 2001; Linville et al., 2004; Hernandez et al., 2007) and, importantly, reduced the hindbrain territory size (Hernandez et al., 2007; data not shown). Significantly, however, excess RA did not change the axial position of the HB/SC transition relative to somites 2/3 (Fig. 8C,D). These results suggest that factors other than RA are required for the alignment of the HB/SC transition relative to the mesoderm and further support the idea that hindbrain territory size specification and alignment are separate processes.

RA interacts with FGF and Wnt pathways to regulate the rostrocaudal position of the hindbrain/spinal cord transition

To investigate the molecular mechanism by which RA indirectly regulates the HB/SC transition, we analyzed the epistatic relationship between the RA pathway and two other signaling pathways, FGF and Wnt, as they regulate neuroectoderm patterning in amniotes (Mühr

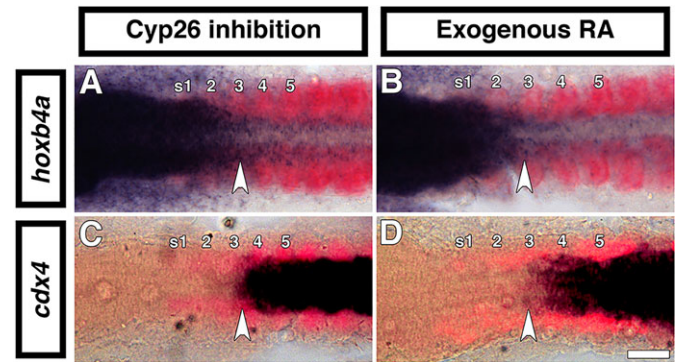


Fig. 8. RA is insufficient to specify the axial position of the HB/SC transition. Excess RA due to inhibition of the RA-degrading enzymes Cyp26 (A,C) or the presence of exogenous RA (B,D) changes the expression of hindbrain but not spinal cord genes (purple). (A,B) Excess RA causes ectopic *hoxb4a* transcription in the hindbrain, but not in the spinal cord. (C,D) Excess RA does not change *cdx4* expression domain. Embryos at 12-somite stage are shown dorsal view, anterior to the left. Arrowheads, somites (s) 2/3 boundary. Scale bar: 50 μm.

et al., 1997, 1999; Ensini et al., 1998; Nordström et al., 2002; Nordström et al., 2006) and are regulated by RA (Zhao and Duester, 2009). We found that RA in zebrafish also regulates the expression of the FGF and Wnt pathway components *etv4* (*pea3*), *wnt3a* and *wnt11*, but not *fgf8* (Fig. 9), making them probable candidates to mediate the indirect activity of RA.

We first investigated the epistatic relationship between FGF and RA, uncovering that they interact in different ways in different processes. With respect to patterning, exposure of gastrula (shield stage) embryos to the FGF receptor inhibitor SU5402 (Mohammadi et al., 1997) caused a reduction in rhombomere size (Fig. 10C; Maves et al., 2002). This phenotype was also observed in FGF/RA-deficient embryos, the only difference being that these embryos also lacked posterior rhombomeres (Fig. 10A–D). Thus, with respect to hindbrain patterning, FGF and RA pathways have additive functions. With respect to the axial position of the HB/SC transition relative to neural landmarks, loss of FGF caused the HB/SC transition to shift caudally, a phenotype that is opposite to that seen in RA-deficient embryos (Fig. 10A–D). Significantly, simultaneous loss of FGF and RA restored the HB/SC transition to an axial position similar to that seen in wild-type embryos (Fig. 10A–D), suggesting that FGF and RA have antagonistic effects in positioning the HB/SC transition. With respect to mesodermal landmarks, however, loss of FGF in wild-type and RA-deficient embryos caused the s2/s3 junction to be situated anterior to the HB/SC transition. Thus, for neural to mesoderm alignment, FGF is epistatic to RA. In this way, FGF and RA interactions are different in each process: additive in hindbrain patterning, antagonistic in hindbrain size specification and epistatic in neural-mesodermal tissue alignment.

We next investigated the epistatic relationship between Wnt and RA, uncovering strong interactions between the two pathways. Loss of Wnt activity due to the activation of a *dkk1-GFP* transgene at gastrulation caused minor rhombomere expansion and caudal shift in the axial position of the HB/SC transition, but did not affect neural-to-mesoderm alignment (Fig. 10E). Strikingly, however, the simultaneous loss of Wnt and RA severely disrupted hindbrain organization and shifted *cdx4* expression caudally (Fig. 10F), suggesting that Wnt and RA act together to regulate *cdx4* and, consequently, the axial positioning of the HB/SC transition. With respect to alignment of tissues, somites in RA/Wnt-deficient

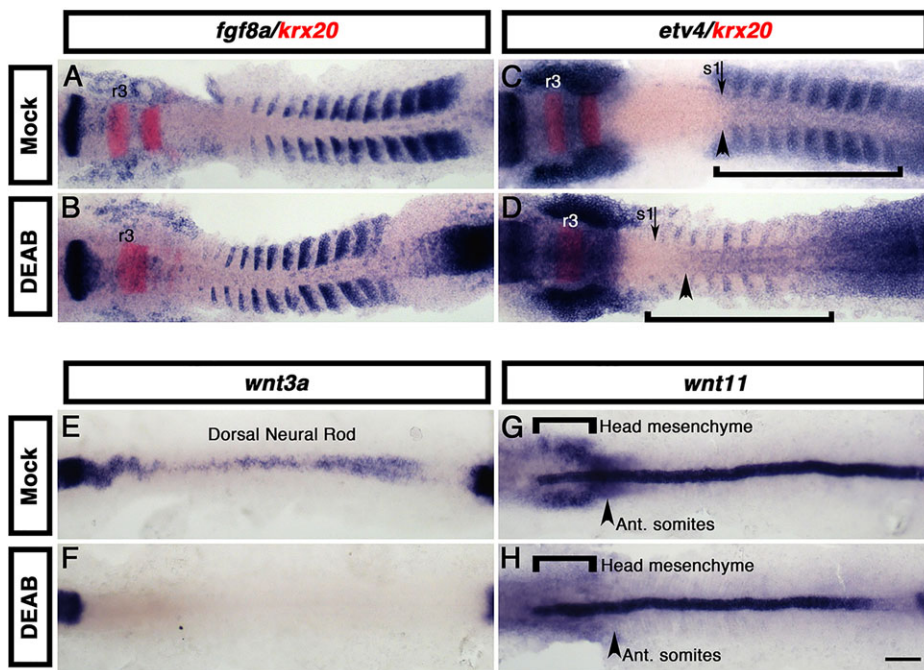


Fig. 9. RA regulates FGF and Wnt pathways. Expression analysis of selected FGF (A–D) and Wnt (E–H) pathway genes (purple) in wild-type (A, C, E, G) and RA-deficient (B, D, F, H) embryos. (A, B) RA loss does not change *FGF8a* expression pattern. (C, D) RA loss changes the transcription of the FGF-pathway target gene *etv4* (*pea3*) in somites (bracket) and spinal cord (arrowhead; axial position relative to somite 1, arrow). (E, F) RA loss abrogates *wnt3a* expression in the dorsal neural tube. (G, H) RA loss downregulates *wnt11* expression in the head mesenchyme (bracket) and anterior somites (arrowhead). Embryos at 12-somite stage are shown dorsal, anterior to the left, and were aligned using the midbrain/hindbrain boundary as a landmark (not labeled). Scale bar: 50 μm.

embryos occupied a more anterior position than in wild-type siblings, a phenotype similar to that observed in RA-deficient embryos. The observations that HB/SC defects associated with the loss of RA were exacerbated by the loss of Wnts suggest that Wnts work downstream or in parallel to RA. Although further work will be required to test these genetic relationships, together our results support a model in which a complex network of interactions between RA, FGF and Wnt signals coordinate the axial position and tissue alignment of the HB/SC and craniovertebral tissues.

DISCUSSION

RA aligns the hindbrain/spinal cord transition to the craniovertebral junction

The alignment of neural and mesodermal tissues at the head-trunk transition requires their development to be coordinated. The present study provides evidence that RA is essential for the accurate alignment of the HB/SC transition to the craniovertebral junction (summarized in Table 1), and that this function is independent from the well-characterized function of RA in hindbrain patterning (Niederreither et al., 1997; Muhr et al., 1999; Begemann et al., 2001; Sakai et al., 2001; Grandel et al., 2002; Kudoh et al., 2002; Emoto et al., 2005; Sirbu et al., 2005; Nordström et al., 2006; Lloret-Vilaspa et al., 2010). Specification of head and trunk territories in zebrafish is completed by mid to late gastrulation (Kim et al., 2002), shortly after prospective hindbrain cells become committed to their fate (Woo and Fraser, 1998) and prospective paraxial mesoderm cells ingress into the embryo, contributing to occipital and anterior vertebral somites (Muller et al., 1996). This is also the critical period during which RA aligns the HB/SC transition to occipital and vertebral somites (Figs 2 and 3). The culmination of this critical period at mid-gastrulation precedes the wave of *hox* gene transcriptional activation that takes place during the second half of gastrulation (Prince et al., 1998; Maves and Kimmel, 2005), thus distinguishing early global and late local neural-to-mesodermal aligning processes. Notably, the novel function of RA in tissue alignment is independent of previously described RA functions in tissue patterning (Muhr et al., 1999; Niederreither et al., 1999; Begemann et al., 2001; Sakai et al., 2001; Grandel et al., 2002;

Kudoh et al., 2002; Emoto et al., 2005; Sirbu et al., 2005; Nordström et al., 2006; Lloret-Vilaspa et al., 2010), as patterning and alignment utilize different genetic cascades (e.g. *hnf1ba* in patterning but not alignment; Fig. 5) and operate in different tissues (autonomous for patterning, non-autonomous for alignment; Fig. 7). In addition, excess RA has different effects on patterning and alignment processes. Whereas excess of RA causes hindbrain patterning defects (Grandel et al., 2002; Maves and Kimmel, 2005), it does not change the alignment of tissues (Fig. 8). We propose that one of the earliest functions of RA at the head-trunk junction is to align the HB/SC transition to occipital and vertebral somites in a Hox-independent manner, but that this function requires additional signals, as RA is necessary but insufficient for the alignment of neural and mesodermal tissues.

RA specifies the size of the hindbrain territory by negatively regulating *Cdx4*

A second novel function of RA is in hindbrain size specification, an activity that is distinct from its functions in tissue alignment and patterning. RA function in territory specification can be distinguished from its function in tissue alignment temporally, with RA being required during the first half of gastrulation for alignment and throughout gastrulation for territory specification (Fig. 2). RA functions in territory specification and patterning can also be distinguished genetically; hindbrain patterning requires *Hnf1ba*, whereas territory specification does not (Fig. 5). Furthermore, territory specification crucially depends on RA restricting the *cdx4* expression domain, as loss of RA reduces the spinal cord territory in a *Cdx4*-dependent manner (Fig. 4). Based on this dependency, we propose that RA regulates the size of the hindbrain territory by establishing in the caudal neural plate an anterior *cdx4*-negative region that can then segment, and a posterior *cdx4*-positive region that will form the spinal cord.

Although the mechanism by which RA negatively regulates *cdx4* is currently unknown, several lines of evidence support the notion of this activity as indirect. In mouse, comparative transcriptome analysis of wild-type and RA-deficient embryos failed to identify *cdx4* as an RA target (Paschaki et al., 2013), whereas in zebrafish,

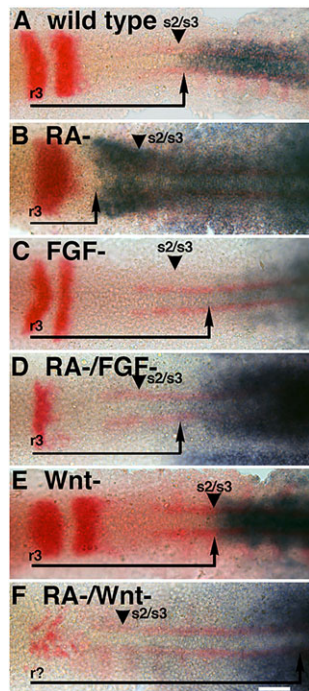


Fig. 10. RA interacts differentially with FGF and Wnts in regulating the axial position of the HB/SC transition. (A) Wild-type expression of *cdx4* (purple) relative to *r2/r3* (*krx20*, red) and somites (*myoD*, red). (B) In RA-deficient embryos, *cdx4* expression shifts rostrally and becomes misaligned. (C) In FGF-deficient embryos, *cdx4* expression shifts caudally and becomes misaligned. (D) In RA/FGF-deficient embryos, *cdx4* expression is similar to wild type relative to *r2/r3*, but misaligned relative to *s2/s3*. (E) In Wnt-deficient embryos, *cdx4* expression shifts caudally relative to *r3* while remaining aligned to *s2/s3*. (F) In RA/Wnt-deficient embryos, *cdx4* expression is dramatically shifted caudally, becoming misaligned. Embryos are at 12-somite stage, dorsal view, anterior to the left. Arrows, distance from *r2/r3* to *cdx4* expression domain; arrowheads, *s2/s3* border. Scale bar: 50 μm .

our transplants show that RA is not required in the nervous system for *cdx4* transcription (Fig. 7). Probable candidates to mediate RA activity are Wnts, which in zebrafish and mouse are under RA regulation (Fig. 9; Zhao and Duester, 2009; Paschaki et al., 2013) and are direct positive regulators of *cdx4* (Shimizu et al., 2005, 2006; Pilon et al., 2006; Lengerke et al., 2011; Ro and Dawid, 2011). RA regulation of Wnts has previously been reported in other developmental contexts, particularly in the mesoderm (reviewed by Wilson et al., 2009; Aulehla and Pourquié, 2010). Based on these observations, we propose that RA regulates *cdx4* expression domain through Wnts to partition the caudal neural plate into hindbrain and spinal cord.

RA and hindbrain patterning

RA is required for hindbrain patterning (Muhr et al., 1999; Niederreither et al., 1999; Begemann et al., 2001; Sakai et al., 2001; Grandel et al., 2002; Kudoh et al., 2002; Emoto et al., 2005; Sirbu et al., 2005; Nordström et al., 2006; Lloret-Vilaspa et al.,

2010); yet, as our experiments show, posterior rhombomeres can develop independently of RA when the hindbrain territory is expanded caudally due to loss of *Cdx4* (Fig. 6). Given that specification of posterior rhombomeres requires RA-dependent activation of *hnf1b* and *hox* genes (Marshall et al., 1994; Gould et al., 1998; Packer et al., 1998; Studer et al., 1998; Zhang et al., 2000; Serpente et al., 2005; Pouilhe et al., 2007), how are posterior rhombomeres in RA/*Cdx4*-deficient embryos being specified? The time at which *Cdx4* specifies the hindbrain and spinal cord territories during gastrulation (Figs 2 and 3) is also the time when the hindbrain is patterned by opposing but partially overlapping FGF and RA gradients (Maves et al., 2002; Roy and Sagerstrom, 2004; Hernandez et al., 2007; Pouilhe et al., 2007; Labalette et al., 2011). Both signals are morphogens (White et al., 2007; Nowak et al., 2011), and each one alone is sufficient for the induction of several rhombomere fates when exogenously applied (Roy and Sagerstrom, 2004). We propose that *Cdx4* constraining the size of the hindbrain territory forces the use of two opposing morphogens for rhombomere patterning. When *Cdx4* is lost, the hindbrain primordium becomes enlarged and the two-morphogen system is no longer necessary for hindbrain patterning. Under these circumstances, the field of hindbrain cells is large enough for a single morphogen, FGF in RA-deficient embryos, to convey to cells their positional information. Whereas further work is needed to demonstrate that a gradient of FGF alone is sufficient for patterning when the hindbrain territory is expanded, this is a viable possibility, given the small size of the hindbrain primordium during gastrulation (Prince et al., 1998; Maves et al., 2002) and the relatively large diffusion coefficient and morphogenetic activity of FGF (Nowak et al., 2011). We propose that during normal development a double morphogenetic gradient is required to pattern the hindbrain as a result of *Cdx* specifying the spinal cord and constraining the hindbrain primordium. Thus, by preventing the specification of spinal cord identities from overtaking the hindbrain territory, aligning the hindbrain territory to mesodermal tissues and patterning the hindbrain, RA functions as a primary regulator of neural and mesodermal tissue organization at the head-trunk transition.

MATERIALS AND METHODS

Zebrafish embryos of stock *AB (wild type), *hnf1ba*^{hi1843} (*vhnf1/tcf2*; Choe et al., 2008), *kgg*^{iv205} (*cdx4*; Davidson et al., 2003), *Tg(zCREST1(isl1):membRFP)* (Mapp et al., 2010), *Tg(isl1:GFP)* (Higashijima et al., 2000), *Tg(olig2:DsRed)* (Kim et al., 2008) and *Tg(hsp70l:dkk1b-GFP)* (Stoick-Cooper et al., 2007) were obtained from natural crosses of adult fish raised and handled according to standard protocols and animal care guidelines (Westerfield, 1994). Embryos were grown at 28°C and staged as previously described (Kimmel et al., 1995). Pharmacological treatments were carried out in embryo media containing 0.1% DMSO (Mallinckrodt) in the dark. To block pigmentation, embryos older than 24 h were treated with 0.003% 1-phenyl-2-thiourea (Sigma-Aldrich) (Westerfield, 1994). Inactivation of FGF and Wnt signaling was performed at shield stage by exposing embryos to 2×10^{-4} M SU5402 (EMD Millipore) (Mohammadi et al., 1997), or by inducing *dkk1* from an *hsp70l:dkk1b-GFP* transgene at 37°C for 1 h (Stoick-Cooper et al., 2007), respectively. To activate the RA pathway, embryos at 50% epiboly were exposed to 1×10^{-7} M all-trans RA (Sigma-Aldrich) or to 1 μM of the Cyp26 inhibitor R115866 (Janssen

Table 1. Summary functions of RA at the head-trunk transition

Process	Time of activity (Figs 2 and 3)	Mechanism of activity (Figs 7 and 8)	Activity requirement (Figs 5 and 10)
Neural-mesodermal alignment	50-75% epiboly (beginning to mid gastrulation)	Indirect	Wnt (downstream or parallel), FGF (upstream)
Hindbrain territory size specification	50-100% epiboly (gastrulation)	Indirect	Wnt (downstream or parallel), FGF (antagonistic)
Hindbrain patterning	50-100% epiboly (gastrulation)	Direct	Hnf1ba-dependent, FGF (additive)

Pharmaceuticals) (Hernandez et al., 2007). To inactivate the RA pathways, embryos were exposed to the RA synthesis inhibitor 4-(Dimethylamino)-benzaldehyde (DEAB; Sigma-Aldrich) at 1×10^{-5} M, or by overexpressing the RA-metabolizing enzyme *Cyp26c1* (Kudoh et al., 2002; Taimi et al., 2004). For overexpression, embryos were injected at the one-cell stage with capped sense mRNA (SP6 mMessage mMachine Kit; Ambion) at 15 pg *egfp* and 375 pg *cyp26c1*, a concentration determined experimentally to induce RA-deficient phenotypes (supplementary material Fig. S1; and data not shown). Bone mineralization analysis was performed by submerging larvae in 0.2% calcein solution as described (Du et al., 2001). Embryos at the appropriate stage were fixed with 4% paraformaldehyde in $1 \times$ PBS pH 7.2 for 3–24 h at 4°C before processing. Specimens for *in situ* hybridization were transferred to 100% methanol and stored at -20°C .

Cell transplantation approaches were carried out as previously described (Ho and Kane, 1990). About 30 cells from a 30% epiboly stage donor embryo injected with either *egfp* or *egfp/cyp26c1* mRNA were transplanted five cell diameters away from the blastula margin of a stage-matched, unlabeled hosts. Host embryos with incorporated donor cells in the nervous system were fixed at 12-somite stage before processing.

Gene expression analysis was carried out by *in situ* hybridization following standard protocols (Bruce et al., 2001; Svoboda et al., 2001). Gene transcripts were detected using NBT/BCIP (EMD-Millipore) or Fast Red (Roche Diagnostics) as enzyme substrates. Proteins were detected using primary antibodies against Myosin heavy chain (Developmental Studies Hybridoma Bank, #A4.1025; 1:500), acetylated Tubulin (Santa Cruz Biotechnology, #6-11B-1; 1:1000) and EGFP (AnaSpec, #29779; 1:500), followed by goat secondary antibodies against mouse IgG2a-Alexa 488, mouse IgG2b-Alexa 568 and rabbit-Alexa 633 (Life Technologies; 1:2000). After 30 min post fixation, embryos were cleared in 70% glycerol or DAPI-Vectashield (Vector Laboratories) and mounted for observation. Specimens were photographed with AxioCam MRc cameras mounted on Zeiss Discovery SteREO V20 or AxioExaminer Z1 microscopes. For confocal imaging, single optical sections of 3 μm thickness and image stacks were obtained using a Leica TCS SP5 confocal microscope. Images were processed using ImageJ 1.49b (NIH). Photos of representative embryos were assembled into figures using Photoshop CS4 extended v11 (Adobe). Unless otherwise noted, all experiments were performed in triplicate, with at least ten embryos per experiment analyzed for a total of $n \geq 30$ embryos, and with at least 95% of embryos displaying the represented phenotype.

Acknowledgements

We thank members of the Skromne laboratory for helpful comments; A. Bruce, J. Baker, A. Foley, J. Chang and R. K. Ho for critically reading the manuscript; R. Cepeda and J. Waite for technical assistance and fish care; B. Apple, K. Higashijima, N. Hopkins, V. Prince and W. Talbot for strains, and the zebrafish community for probes and reagents. The Hybridoma Bank is maintained by The University of Iowa under NICHHD auspices.

Competing interests

The authors declare no competing financial interests.

Author contributions

K.L. and I.S. designed, performed and analyzed the experiments. I.S. wrote the manuscript.

Funding

This study was supported by the University of Miami's College of Arts and Sciences, Neuroscience Program and Provost Award, and by a National Science Foundation grant [IOS-090449].

Supplementary material

Supplementary material available online at <http://dev.biologists.org/lookup/suppl/doi:10.1242/dev.109603/-DC1>

References

Aulehla, A. and Pourquie, O. (2010). Signaling gradients during paraxial mesoderm development. *CSH Perspect. Biol.* **2**, a000869.

Beck, F., Erler, T., Russell, A. and James, R. (1995). Expression of *Cdx-2* in the mouse embryo and placenta: possible role in patterning of the extra-embryonic membranes. *Dev. Dyn.* **204**, 219–227.

Begemann, G., Schilling, T. F., Rauch, G. J., Geisler, R. and Ingham, P. W. (2001). The zebrafish neckless mutation reveals a requirement for *raldh2* in mesodermal signals that pattern the hindbrain. *Development* **128**, 3081–3094.

Brown, J. M. and Storey, K. G. (2000). A region of the vertebrate neural plate in which neighbouring cells can adopt neural or epidermal fates. *Curr. Biol.* **10**, 869–872.

Bruce, A. E. E., Oates, A. C., Prince, V. E. and Ho, R. K. (2001). Additional *hox* clusters in the zebrafish: divergent expression patterns belie equivalent activities of duplicate *hoxB5* genes. *Evol. Devel.* **3**, 127–144.

Charite, J., de Graaff, W., Consten, D., Reijnen, M. J., Korving, J. and Deschamps, J. (1998). Transducing positional information to the *Hox* genes: critical interaction of *cdx* gene products with position-sensitive regulatory elements. *Development* **125**, 4349–4358.

Choe, S.-K., Hirsch, N., Zhang, X. and Sagerström, C. G. (2008). *hnf1b* genes in zebrafish hindbrain development. *Zebrafish* **5**, 179–187.

Davidson, A. J., Ernst, P., Wang, Y., Dekens, M. P. S., Kingsley, P. D., Palis, J., Korsmeyer, S. J., Daley, G. Q. and Zon, L. I. (2003). *cdx4* mutants fail to specify blood progenitors and can be rescued by multiple *hox* genes. *Nature* **425**, 300–306.

Deschamps, J. and van Nes, J. (2005). Developmental regulation of the *Hox* genes during axial morphogenesis in the mouse. *Development* **132**, 2931–2942.

Du, S. J., Frenkel, V., Kindschi, G. and Zohar, Y. (2001). Visualizing normal and defective bone development in zebrafish embryos using the fluorescent chromophore calcein. *Dev. Biol.* **238**, 239–246.

Emoto, Y., Wada, H., Okamoto, H., Kudo, A. and Imai, Y. (2005). Retinoic acid-metabolizing enzyme *Cyp26a1* is essential for determining territories of hindbrain and spinal cord in zebrafish. *Dev. Biol.* **278**, 415–427.

Ensign, M., Tsuchida, T. N., Belting, H. G. and Jessell, T. M. (1998). The control of rostrocaudal pattern in the developing spinal cord: specification of motor neuron subtype identity is initiated by signals from paraxial mesoderm. *Development* **125**, 969–982.

Frumkin, A., Rangini, Z., Ben-Yehuda, A., Gruenbaum, Y. and Fainsod, A. (1991). A chicken caudal homologue, *CHox-cad*, is expressed in the epiblast with posterior localization and in the early endodermal lineage. *Development* **112**, 207–219.

Gamer, L. W. and Wright, C. V. E. (1993). Murine *Cdx-4* bears striking similarities to the *Drosophila* caudal gene in its homeodomain sequence and early expression pattern. *Mech. Dev.* **43**, 71–81.

Glover, J. C., Renaud, J.-S. and Rijli, F. M. (2006). Retinoic acid and hindbrain patterning. *J. Neurobiol.* **66**, 705–725.

Gould, A., Itasaki, N. and Krumlauf, R. (1998). Initiation of rhombomeric *Hoxb4* expression requires induction by somites and a retinoid pathway. *Neuron* **21**, 39–51.

Grandel, H., Lun, K., Rauch, G. J., Rhinn, M., Piotrowski, T., Houart, C., Sordino, P., Kuchler, A. M., Schulte-Merker, S., Geisler, R. et al. (2002). Retinoic acid signalling in the zebrafish embryo is necessary during pre-segmentation stages to pattern the anterior-posterior axis of the CNS and to induce a pectoral fin bud. *Development* **129**, 2851–2865.

Hernandez, R. E., Rikhof, H. A., Bachmann, R. and Moens, C. B. (2004). *vhnf1* integrates global RA patterning and local FGF signals to direct posterior hindbrain development in zebrafish. *Development* **131**, 4511–4520.

Hernandez, R. E., Putzke, A. P., Myers, J. P., Margaretha, L. and Moens, C. B. (2007). *Cyp26* enzymes generate the retinoic acid response pattern necessary for hindbrain development. *Development* **134**, 177–187.

Higashijima, S., Hotta, Y. and Okamoto, H. (2000). Visualization of cranial motor neurons in live transgenic zebrafish expressing green fluorescent protein under the control of the *islet-1* promoter/enhancer. *J. Neurosci.* **20**, 206–218.

Hill, J., Clarke, J. D. W., Vargesson, N., Jowett, T. and Holder, N. (1995). Exogenous retinoic acid causes specific alterations in the development of the midbrain and hindbrain of the zebrafish embryo including positional respecification of the Mauthner neuron. *Mech. Dev.* **50**, 3–16.

Ho, R. K. and Kane, D. A. (1990). Cell-autonomous action of zebrafish *spt-1* mutation in specific mesodermal precursors. *Nature* **348**, 728–730.

Kim, S. H., Shin, J., Park, H. C., Yeo, S. Y., Hong, S. K., Han, S., Rhee, M., Kim, C. H., Chitnis, A. B. and Huh, T. L. (2002). Specification of an anterior neuroectoderm patterning by Frizzled8a-mediated *Wnt8b* signalling during late gastrulation in zebrafish. *Development* **129**, 4443–4455.

Kim, H., Shin, J., Kim, S., Poling, J., Park, H.-C. and Appel, B. (2008). Notch-regulated oligodendrocyte specification from radial glia in the spinal cord of zebrafish embryos. *Dev. Dyn.* **237**, 2081–2089.

Kimmel, C. B., Ballard, W. W., Kimmel, S. R., Ullmann, B. and Schilling, T. F. (1995). Stages of embryonic development of the zebrafish. *Dev. Dyn.* **203**, 253–310.

Kudoh, T., Wilson, S. W. and Dawid, I. B. (2002). Distinct roles for *Fgf*, *Wnt* and retinoic acid in posteriorizing the neural ectoderm. *Development* **129**, 4335–4346.

Labalette, C., Bouchoucha, Y. X., Wassef, M. A., Gongal, P. A., Le Men, J., Becker, T., Gilardi-Hebenstreit, P. and Charnay, P. (2011). Hindbrain patterning requires fine-tuning of early *krox20* transcription by *Sprouty 4*. *Development* **138**, 317–326.

- Lengerke, C., Wingert, R., Beeretz, M., Grauer, M., Schmidt, A. G., Konantz, M., Daley, G. Q. and Davidson, A. J. (2011). Interactions between *cdx* genes and retinoic acid modulate early cardiogenesis. *Dev. Biol.* **354**, 134–142.
- Linville, A., Gumusaneli, E., Chandraratna, R. A. S. and Schilling, T. F. (2004). Independent roles for retinoic acid in segmentation and neuronal differentiation in the zebrafish hindbrain. *Dev. Biol.* **270**, 186–199.
- List, C. F. (1941). Neurologic syndromes accompanying developmental anomalies of occipital bone, atlas and axis. *Arch. Neurol. Psy.* **45**, 577–616.
- Liu, J.-P., Laufer, E. and Jessell, T. M. (2001). Assigning the positional identity of spinal motor neurons: rostrocaudal patterning of Hox-c expression by FGFs, Gdf11, and retinoids. *Neuron* **32**, 997–1012.
- Lloret-Vilaspa, F., Jansen, H. J., de Roos, K., Chandraratna, R. A. S., Zile, M. H., Stern, C. D. and Durston, A. J. (2010). Retinoid signalling is required for information transfer from mesoderm to neuroectoderm during gastrulation. *Int. J. Dev. Biol.* **54**, 599–608.
- Lohnes, D. (2003). The Cdx1 homeodomain protein: an integrator of posterior signaling in the mouse. *Bioessays* **25**, 971–980.
- Mapp, O. M., Wanner, S. J., Rohrschneider, M. R. and Prince, V. E. (2010). Prickle1b mediates interpretation of migratory cues during zebrafish facial branchiomotor neuron migration. *Dev. Dyn.* **239**, 1596–1608.
- Marin-Padilla, M. (1991). Cephalic axial skeletal-neural dysraphic disorders: embryology and pathology. *Can. J. Neurol. Sci.* **18**, 153–169.
- Marshall, H., Studer, M., Pöpperl, H., Aparicio, S., Kuroiwa, A., Brenner, S. and Krumlauf, R. (1994). A conserved retinoic acid response element required for early expression of the homeobox gene *Hoxb-1*. *Nature* **370**, 567–571.
- Maves, L. and Kimmel, C. B. (2005). Dynamic and sequential patterning of the zebrafish posterior hindbrain by retinoic acid. *Dev. Biol.* **285**, 593–605.
- Maves, L., Jackman, W. and Kimmel, C. B. (2002). FGF3 and FGF8 mediate a rhombomere 4 signaling activity in the zebrafish hindbrain. *Development* **129**, 3825–3837.
- Meyer, B. I. and Gruss, P. (1993). Mouse *Cdx-1* expression during gastrulation. *Development* **117**, 191–203.
- Mohammadi, M., McMahon, G., Sun, L., Tang, C., Hirth, P., Yeh, B. K., Hubbard, S. R. and Schlessinger, J. (1997). Structures of the tyrosine kinase domain of fibroblast growth factor receptor in complex with inhibitors. *Science* **276**, 955–960.
- Morin-Kensicki, E. M., Melancon, E. and Eisen, J. S. (2002). Segmental relationship between somites and vertebral column in zebrafish. *Development* **129**, 3851–3860.
- Muhr, J., Jessell, T. M. and Edlund, T. (1997). Assignment of early caudal identity to neural plate cells by a signal from caudal paraxial mesoderm. *Neuron* **19**, 487–502.
- Muhr, J., Graziano, E., Wilson, S., Jessell, T. M. and Edlund, T. (1999). Convergent inductive signals specify midbrain, hindbrain, and spinal cord identity in gastrula stage chick embryos. *Neuron* **23**, 689–702.
- Muller, M., v Weizsacker, E. and Campos-Ortega, J. A. (1996). Expression domains of a zebrafish homologue of the *Drosophila* pair-rule gene *hairy* correspond to primordia of alternating somites. *Development* **122**, 2071–2078.
- Niederreither, K., McCaffery, P., Dräger, U. C., Chambon, P. and Dollé, P. (1997). Restricted expression and retinoic acid-induced downregulation of the retinaldehyde dehydrogenase type 2 (RALDH-2) gene during mouse development. *Mech. Dev.* **62**, 67–78.
- Niederreither, K., Subbarayan, V., Dollé, P. and Chambon, P. (1999). Embryonic retinoic acid synthesis is essential for early mouse post-implantation development. *Nat. Genet.* **21**, 444–448.
- Nordström, U., Jessell, T. M. and Edlund, T. (2002). Progressive induction of caudal neural character by graded Wnt signaling. *Nat. Neurosci.* **5**, 525–532.
- Nordström, U., Maier, E., Jessell, T. M. and Edlund, T. (2006). An early role for Wnt signaling in specifying neural patterns of *Cdx* and *Hox* gene expression and motor neuron subtype identity. *PLoS Biol.* **4**, e252.
- Nowak, M., Machate, A., Yu, S. R., Gupta, M. and Brand, M. (2011). Interpretation of the FGF8 morphogen gradient is regulated by endocytic trafficking. *Nat. Cell Biol.* **13**, 153–158.
- Oxtoby, E. and Jowett, T. (1993). Cloning of the zebrafish *krox-20* gene (*krx-20*) and its expression during hindbrain development. *Nucleic Acids Res.* **21**, 1087–1095.
- Packer, A. I., Crotty, D. A., Elwell, V. A. and Wolgemuth, D. J. (1998). Expression of the murine *Hoxa4* gene requires both autoregulation and a conserved retinoic acid response element. *Development* **125**, 1991–1998.
- Paschaki, M., Schneider, C., Rhinn, M., Thibault-Carpentier, C., Dembélé, D., Niederreither, K. and Dollé, P. (2013). Transcriptomic analysis of murine embryos lacking endogenous retinoic acid signaling. *PLoS ONE* **8**, e62274.
- Pilon, N., Oh, K., Sylvestre, J.-R., Bouchard, N., Savory, J. and Lohnes, D. (2006). *Cdx4* is a direct target of the canonical Wnt pathway. *Dev. Biol.* **289**, 55–63.
- Pouilhe, M., Gilardi-Hebenstreit, P., Desmarquet-Trin Dinh, C. and Charnay, P. (2007). Direct regulation of *vHnf1* by retinoic acid signaling and MAF-related factors in the neural tube. *Dev. Biol.* **309**, 344–357.
- Prince, V. E., Moens, C. B., Kimmel, C. B. and Ho, R. K. (1998). Zebrafish *hox* genes: expression in the hindbrain region of wild-type and mutants of the segmentation gene, *valentino*. *Development* **125**, 393–406.
- Rhinn, M. and Dollé, P. (2012). Retinoic acid signalling during development. *Development* **139**, 843–858.
- Ro, H. and Dawid, I. B. (2011). Modulation of Tcf3 repressor complex composition regulates *cdx4* expression in zebrafish. *EMBO J.* **30**, 2894–2907.
- Roy, N. M. and Sagerström, C. G. (2004). An early Fgf signal required for gene expression in the zebrafish hindbrain primordium. *Dev. Brain Res.* **148**, 27–42.
- Sakai, Y., Meno, C., Fujii, H., Nishino, J., Shiratori, H., Saijoh, Y., Rossant, J. and Hamada, H. (2001). The retinoic acid-inactivating enzyme CYP26 is essential for establishing an uneven distribution of retinoic acid along the anterior-posterior axis within the mouse embryo. *Genes Dev.* **15**, 213–225.
- Schoenwolf, G. C. (1992). Morphological and mapping studies of the paranodal and postnodal levels of the neural plate during chick neurulation. *Anat. Rec.* **233**, 281–290.
- Serpente, P., Tumpel, S., Ghyselincx, N. B., Niederreither, K., Wiedemann, L. M., Dollé, P., Chambon, P., Krumlauf, R. and Gould, A. P. (2005). Direct crossregulation between retinoic acid receptor {beta} and *Hox* genes during hindbrain segmentation. *Development* **132**, 503–513.
- Shimizu, T., Bae, Y.-K., Muraoka, O. and Hibi, M. (2005). Interaction of Wnt and caudal-related genes in zebrafish posterior body formation. *Dev. Biol.* **279**, 125–141.
- Shimizu, T., Bae, Y.-K. and Hibi, M. (2006). *Cdx-Hox* code controls competence for responding to Fgfs and retinoic acid in zebrafish neural tissue. *Development* **133**, 4709–4719.
- Sirbu, I. O., Gresh, L., Barra, J. and Duester, G. (2005). Shifting boundaries of retinoic acid activity control hindbrain segmental gene expression. *Development* **132**, 2611–2622.
- Skromne, I., Thorsen, D., Hale, M., Prince, V. E. and Ho, R. K. (2007). Repression of the hindbrain developmental program by *Cdx* factors is required for the specification of the vertebrate spinal cord. *Development* **134**, 2147–2158.
- Sockanathan, S. and Jessell, T. M. (1998). Motor neuron-derived retinoid signaling specifies the subtype identity of spinal motor neurons. *Cell* **94**, 503–514.
- Stern, C. D., Charite, J., Deschamps, J., Duboule, D., Durston, A. J., Kmita, M., Nicolas, J.-F., Palmeirim, I., Smith, J. C. and Wolpert, L. (2006). Head-tail patterning of the vertebrate embryo: one, two or many unresolved problems? *Int. J. Dev. Biol.* **50**, 3–15.
- Stoick-Cooper, C. L., Weidinger, G., Riehle, K. J., Hubbert, C., Major, M. B., Fausto, N. and Moon, R. T. (2007). Distinct Wnt signaling pathways have opposing roles in appendage regeneration. *Development* **134**, 479–489.
- Studer, M., Gavallas, A., Marshall, H., Ariza-McNaughton, L., Rijli, F. M., Chambon, P. and Krumlauf, R. (1998). Genetic interactions between *Hoxa1* and *Hoxb1* reveal new roles in regulation of early hindbrain patterning. *Development* **125**, 1025–1036.
- Sturgeon, K., Kaneko, T., Biemann, M., Gauthier, A., Chawengsaksohak, K. and Cordes, S. P. (2011). *Cdx1* refines positional identity of the vertebrate hindbrain by directly repressing *Mafb* expression. *Development* **138**, 65–74.
- Sun, Z. and Hopkins, N. (2001). *vhnf1*, the *MODY5* and familial GCKD-associated gene, regulates regional specification of the zebrafish gut, pronephros, and hindbrain. *Genes Dev.* **15**, 3217–3229.
- Svoboda, K. R., Linares, A. E. and Ribera, A. B. (2001). Activity regulates programmed cell death of zebrafish Rohon-Beard neurons. *Development* **128**, 3511–3520.
- Swindell, E. C., Thaller, C., Sockanathan, S., Petkovich, M., Jessell, T. M. and Eichele, G. (1999). Complementary domains of retinoic acid production and degradation in the early chick embryo. *Dev. Biol.* **216**, 282–296.
- Taimi, M., Helvig, C., Wisniewski, J., Ramshaw, H., White, J., Amad, M., Korczak, B. and Petkovich, M. (2004). A novel human cytochrome P450, CYP26C1, involved in metabolism of 9-cis and all-trans isomers of retinoic acid. *J. Biol. Chem.* **279**, 77–85.
- van Rooijen, C., Simmini, S., Bialecka, M., Neijts, R., van de Ven, C., Beck, F. and Deschamps, J. (2012). Evolutionarily conserved requirement of *Cdx* for post-occipital tissue emergence. *Development* **139**, 2576–2583.
- Weinberg, E. S., Allende, M. L., Kelly, C. S., Abdelhamid, A., Murakami, T., Andermann, P., Doerre, O. G., Grunwald, D. J. and Riggelman, B. (1996). Developmental regulation of zebrafish *MyoD* in wild-type, no tail and spadetail embryos. *Development* **122**, 271–280.
- Westerfield, M. (1994). *The zebrafish book: a guide for the laboratory use of zebrafish (Danio rerio)*. Eugene, OR: University of Oregon Press.
- White, R. J., Nie, Q., Lander, A. D. and Schilling, T. F. (2007). Complex regulation of *cyp26a1* creates a robust retinoic acid gradient in the zebrafish embryo. *PLoS Biol.* **5**, e304.
- Wiellette, E. L. and Sive, H. (2003). *vhnf1* and Fgf signals synergize to specify rhombomere identity in the zebrafish hindbrain. *Development* **130**, 3821–3829.
- Wilson, V., Olivera-Martinez, I. and Storey, K. G. (2009). Stem cells, signals and vertebrate body axis extension. *Development* **136**, 1591–1604.
- Woo, K. and Fraser, S. (1998). Specification of the hindbrain fate in the zebrafish. *Dev. Biol.* **197**, 283–296.
- Zhang, F., Nagy Kovács, E. and Featherstone, M. S. (2000). Murine *hoxd4* expression in the CNS requires multiple elements including a retinoic acid response element. *Mech. Dev.* **96**, 79–89.
- Zhao, X. and Duester, G. (2009). Effect of retinoic acid signaling on Wnt/beta-catenin and FGF signaling during body axis extension. *Gene Expr. Patterns* **9**, 430–435.

SUPPLEMENTARY FIGURE LEGEND

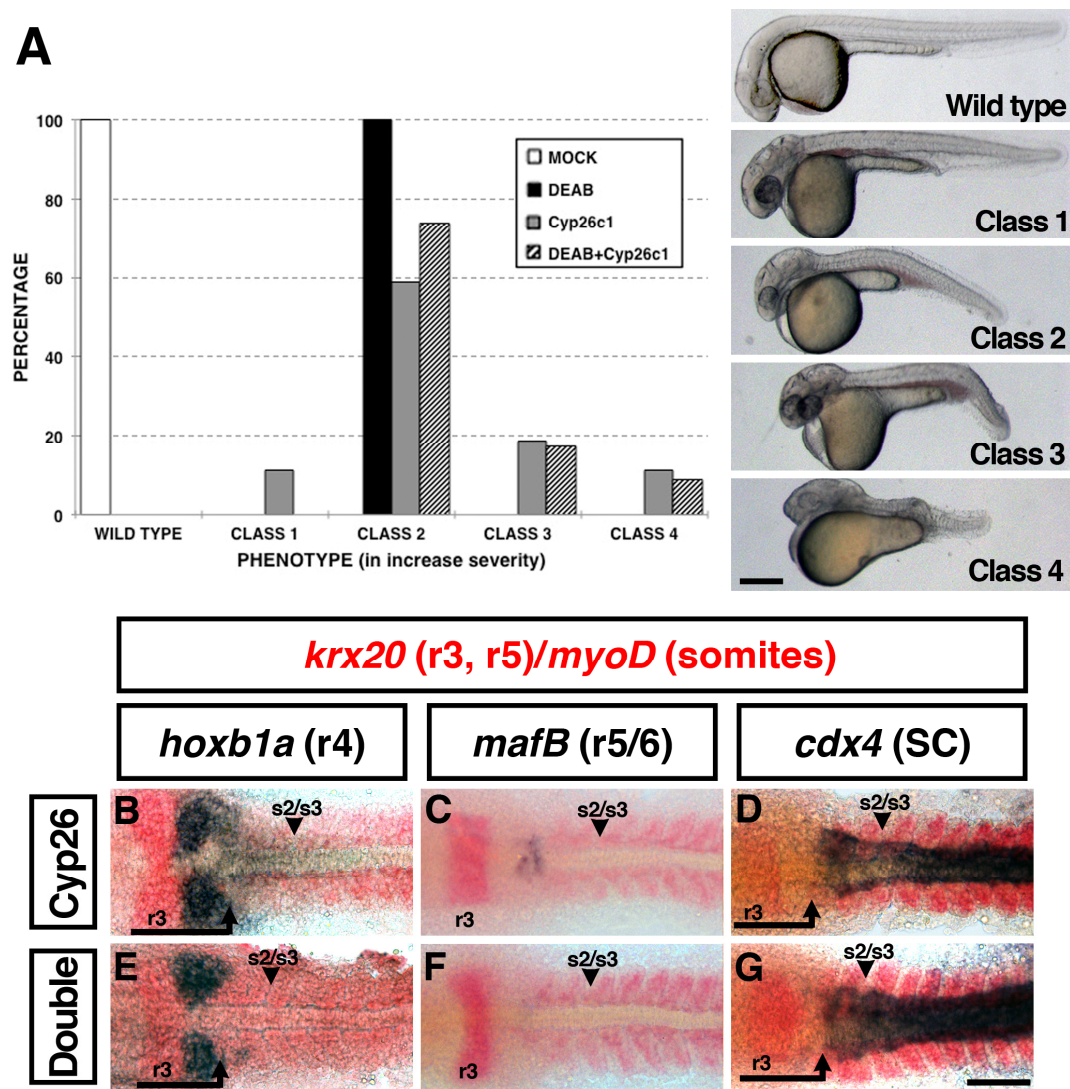


Figure S1. Overexpression of the Retinoic Acid-degrading enzyme Cyp26c1 recapitulates defects associated with loss of Retinoic Acid synthesis. (A) Frequency distribution of morphological defects caused by RA loss due to exposure to the RA synthesis inhibitor DEAB at 50% epiboly (black bars), overexpression of RA-degrading enzyme Cyp26c1 (gray bars) and both (hatched bars). Embryos were scored at 32 hpf using a four-class scale of increase severity. Class 1 had blood pooling. Class 2 had hindbrain size reduction, tail defects, lack of fin buds and edema. Class 3 had severe tail bending. Class 4 had a severely reduced axis and small somites. For each condition, $n=80$ embryos from three independent trials. Cyp26c1 treatments were statistically significant from mock control (white bar), but not DEAB treatments by pairwise chi square analysis (mock versus *cyp26c1* treatment, $\chi^2=63$, $df=1$, $P=0$; DEAB versus *cyp26c1* treatment, $\chi^2=1.01$, $df=1$, $P<0.314$). Embryos are mounted laterally, anterior to the left. Scale bar: 250 μ m. (B-G) Expression analysis of *hoxb1a* (r4; B,E), *mafB* (r5/r6; C,F) and *cdx4*

(spinal cord; D,G) (purple) relative to r2/r3 (*krx20*, red) and somites 2/3 (*myoD*, red) boundaries, in *Cyp26c1*-overexpressing embryos that were not exposed (*Cyp26c1*; B-D) or exposed (Double; E-G) to the RA synthesis inhibitor DEAB. Similar changes were observed in DEAB-treated embryos (Fig. 1). Embryos at 12-somite stage are shown in dorsal view, anterior to the left. Arrows, distance from r2/r3 to the expression domain of the indicated gene; arrowheads, s2/s3 border. Scale bars: 50 μm .